Distance Relay Response to Transformer Energization: Problems and Solutions

Joe Mooney, P.E. and Satish Samineni, Schweitzer Engineering Laboratories

Abstract— **Modern distance relays use various filtering algorithms to extract the fundamental frequency component of power system voltage and current waveforms. The relays then use the filtered voltages and currents in such numerous algorithms as distance, overcurrent, under/overvoltage, and frequency. Use of filtered voltages and currents generally provides a protective relay immunity to power system harmonics such as those resulting from transformer energization. This paper focuses on the application of distance relays on or near power transformers. It reviews digital filtering algorithms and shows both digital filter and distance element algorithm responses to power transformer inrush. Without careful setting of digital relays in such applications, power transformer inrush can cause distance relay measurement errors and unwanted operations.**

This paper provides guidelines for setting distance relays applied directly on a power transformer and for applications of relays to a line on which transformers are connected. The paper demonstrates these guidelines through the use of actual power system events and events modeled on a real-time digital simulator.

I. Review of Digital Relay Filtering Techniques

Digital, or microprocessor-based, relays use various filters to extract the fundamental frequency component of power system waveforms. Analog low-pass filters remove high-frequency components and prevent aliasing of high-frequency signals. Digital filters extract the fundamental frequency component of the voltage and current waveforms. The relays then use these digitally filtered values as phasors in such elements as distance, overcurrent, and over/undervoltage.

The most common digital filters are cosine and Fourier filters [1]. Equation 1 shows a typical implementation of a cosine filter, while Equation 2 shows a typical implementation of a sine filter. A Fourier filter consists of both the sine and cosine filters, whereas a cosine filter consists of only the cosine filter.

$$V_f = \frac{2}{SPC}\sum_{k=0}^{SPC-1}\cos\left(\frac{k \bullet 2\pi}{SPC}\right) \bullet V_{[f-(SPC-1)]+k} \qquad (1)$$

$$V_f = \frac{2}{SPC}\sum_{k=0}^{SPC-1}\sin\left(\frac{k \bullet 2\pi}{SPC}\right) \bullet V_{[f-(SPC-1)]+k} \qquad (2)$$

Where:

V_f is present filtered sample
SPC is number of samples per cycle

To better understand the filter response, we evaluate two outputs of the digital filter: the frequency response and the impulse response. These two responses provide very useful information for evaluating digital filter response to transients and harmonics. We plot the frequency response by applying an input signal at various frequencies and measuring the magnitude of the output. The impulse response is effectively the filter coefficients.

Fig. 1 shows the frequency response of full-cycle cosine and sine filters at 16 samples per cycle. Fig. 2 shows the filter coefficients for the same filters.

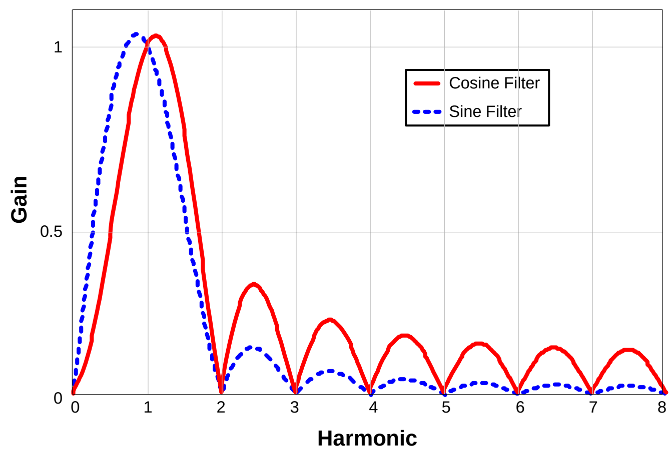

Fig. 1. Frequency Response

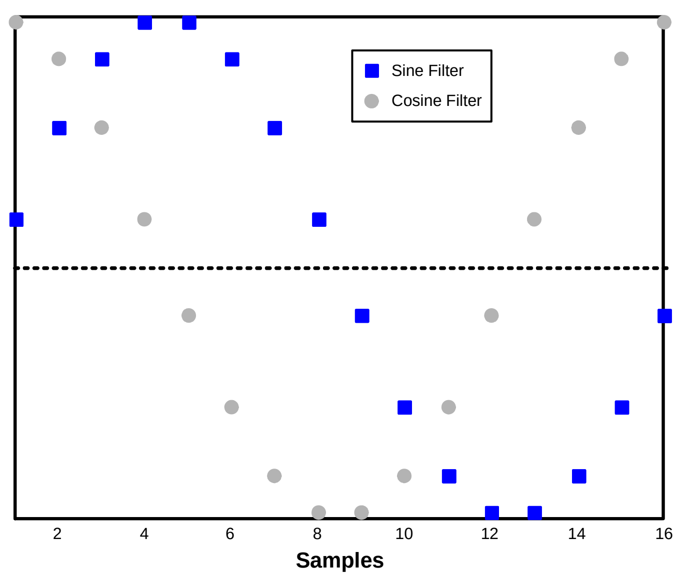

Fig. 2. Filter Coefficients

Evaluation of the filter response to an impulse can be informative. In many ways, an impulse is representative of the currents associated with a transformer inrush condition. Fig. 3 shows the response of a full-cycle cosine filter to a single sample impulse. Note that a single sample impulse provides an output that represents an ac waveform.

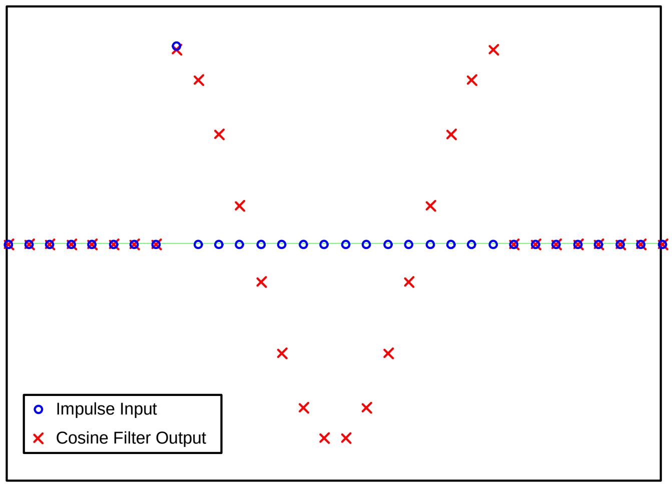

Fig. 3. Impulse Response

II. Digital Filter Response to Transformer Inrush

Transformer inrush is very rich in harmonics and waveform distortion. The distortion occurs primarily on currents; voltages are affected slightly.

Fig. 4 shows typical inrush current waveforms. Fig. 5 shows a magnified view of the first few cycles of data.

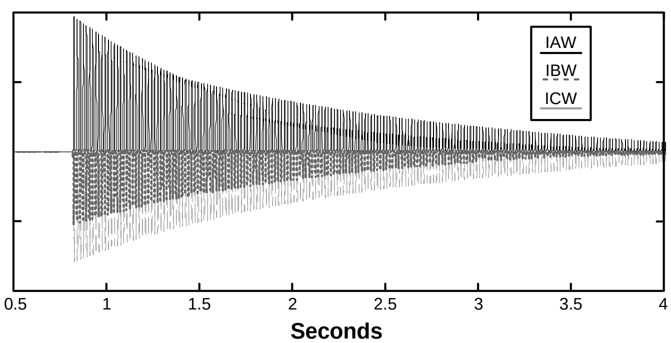

Fig. 4. Typical Inrush Waveforms

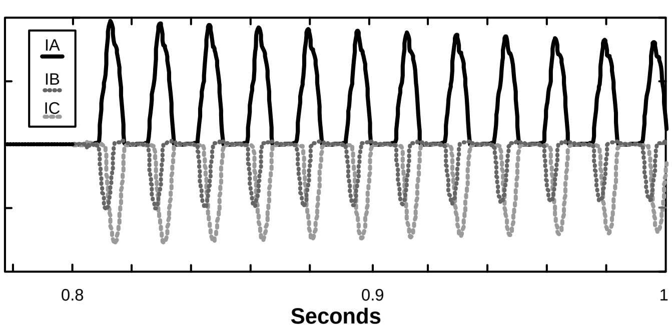

Fig. 5. Inrush Currents – Zoomed-in

Fig. 6 is a fast Fourier transform of the B-phase transformer inrush current. The figure shows all harmonic currents normalized to the fundamental frequency and displayed as a percentage of the fundamental current. Note that the second harmonic content is very high as a percentage of the fundamental current. The third and fourth harmonics are also relatively high. Fifth and greater harmonics are a very small percentage of the total waveform. Note also that the B-phase current has the lowest peak value of inrush current, which may explain the high B-phase content of 2^{nd} and 3^{rd} harmonics. The A-phase and C-phase currents also contain harmonics, but the harmonic content is not as high in relationship to fundamental current as for B-phase.

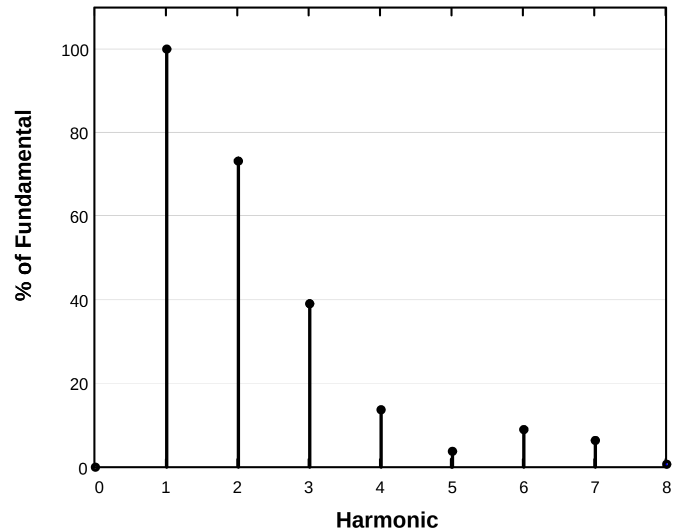

Fig. 6. Harmonic Analysis of Inrush Currents

The digital filter output resembles an ac waveform with a decaying peak magnitude over time. For the cosine filter impulse response, remember that the inrush current is effectively a series of impulses that, after digital filtering with a cosine or sine filter, resembles an ac waveform. This is important for evaluating performance of a distance (or overcurrent) relay.

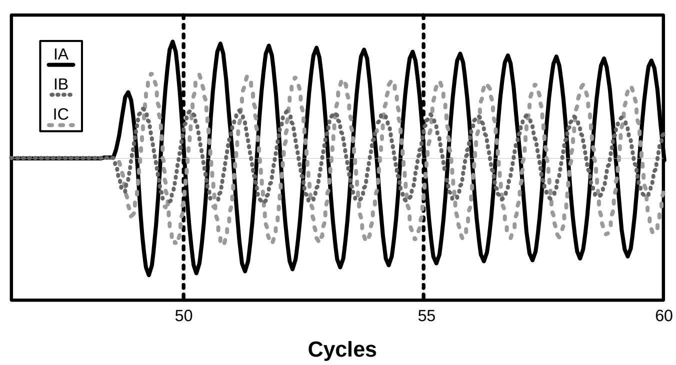

Fig. 7. Output of Full-Cycle Cosine Filter

The cosine filter extracts the fundamental frequency component from the input signals and rejects all harmonic. This is useful for application of distance and overcurrent relays, for which settings are based upon line impedances, and fault calculations that assume fundamental frequency. Although the digital filter rejects inrush current harmonics, there still exists a significant fundamental frequency component. Fig. 8 shows the phase current magnitudes. The maximum value of the A-phase current is nearly 35 percent of the maximum value in Fig. 5.

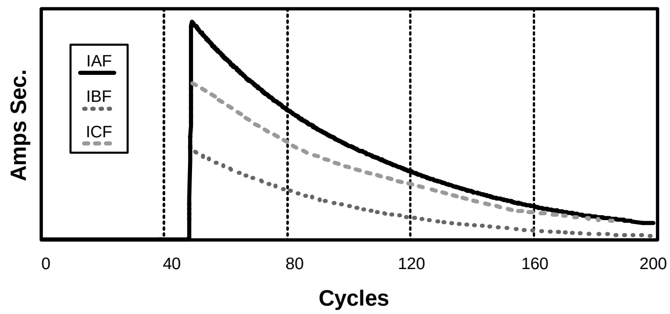

Fig. 8. Magnitude of Filtered Currents

III. Distance Element Review

Distance relays operate by measuring the phase relationship between an operating quantity and a polarizing quantity [2]. The operating quantity, typically known as the line-drop-compensated voltage, consists of the measured voltage, the measured current, and the reach setting. One would typically select a polarizing quantity that would be unaffected by a fault; typical polarizing quantities for mho elements are positive-sequence voltage or unfaulted phase voltage. Equation 3 shows the typical distance element operating equation. Fig. 9 shows the vector relationship.

$$P = \mathrm{Re}\left[\left(r \bullet Z \bullet I - V\right) \bullet V_P^*\right] \tag{3}$$

Where:

P = Operating torque; positive is operate, negative is restrain

r = set reach

Z = replica line impedance

I = measured current

V = measured voltage

Vp = polarizing voltage

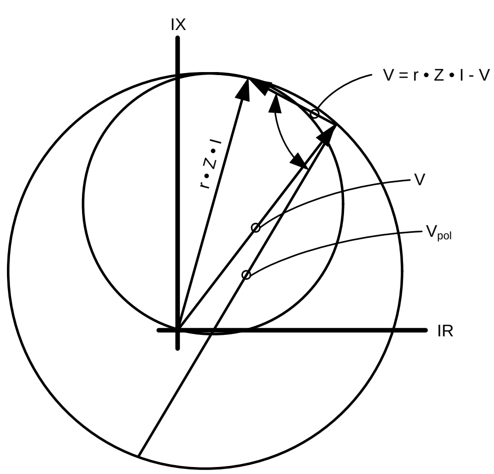

Fig. 9. Mho Element Derivation

Schweitzer and Roberts [2] proposed a novel approach in which manipulation of Equation 3 provides a scalar output representing the term "r". This approach is computationally efficient, in that only a single calculation is necessary per fault loop. The distance element plots in the remainder of this paper use this approach. Note that, when measured impedance is less than the threshold, the distance element operates. Fig. 10 shows an example plot of a fault near the Zone 1 reach.

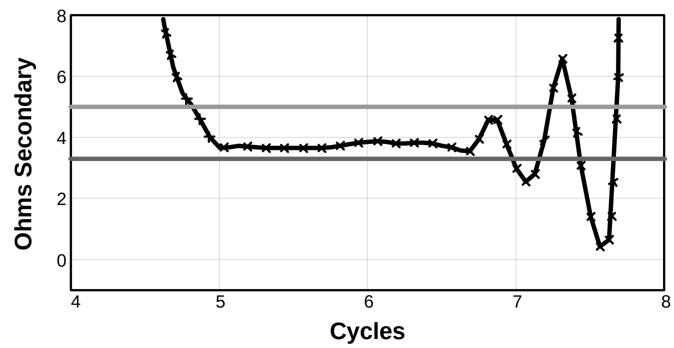

Fig. 10. Example Impedance Plot

Other distance element operation considerations include polarizing voltage and frequency tracking. To ensure correct distance element operation, most relays retain the polarizing voltage value in memory for a set duration. This memory voltage is necessary to ensure that the distance element has polarizing voltage for sufficient time to operate for a zero-voltage fault. Various methods, including use of fixed timers, user settable timers, and infinite impulse response filters, exist for extending the polarizing voltage duration. Occasionally, these memory functions cause a phase shift between the measured quantities and the memorized quantities. This phase shift can result in measurement errors and overreach.

Most digital relays sample at a rate dependent upon the power system frequency, and this rate is typically a fixed number of samples per power system cycle. The relay must therefore adjust the sampling rate when the power system frequency changes. This adjustment is known as frequency tracking. Understanding how a relay tracks frequency can be important, because transformer inrush can result in waveform distortion that causes errors in some frequency tracking algorithms. When the sampling frequency and system frequency do not match, the distance element measurement may be in error.

IV. Application Examples

This section highlights two common distance relay applications that can be subject to transformer inrush.

1. Dedicated transformer
2. Multiple tapped transformers on a transmission line

A. Dedicated Transformer

This example illustrates the distance element response to transformer energization when the relay is applied on the terminals of a 230/23 kV, 240 MVA, three-phase transformer. The transformer is delta connected on the 230 kV side and wye grounded on the 23 kV side. The transformer impedance is 7%. The transformer and system are modeled through the use of an RTDS® Technologies real-time digital simulator. The transformer is configured as a saturable transformer, to model the inrush characteristic properly. To maximize the inrush effect, the transformer is energized at a voltage zero-crossing of the A-phase voltage. There were multiple shots; this example uses the waveform with the greatest magnitude of inrush current.

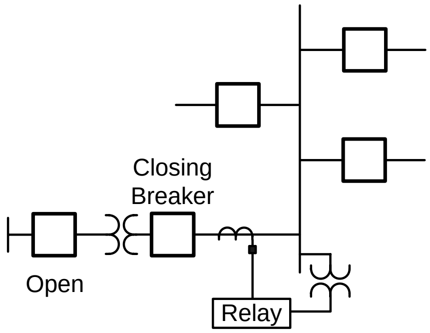

Fig. 11. Single Transformer System Diagram

Fig. 12 shows the inrush currents the simulator captured. Fig. 13 shows the output of the digital filter at 16 samples/cycle. Fig. 14 shows the phase current magnitudes from the digital filter output. Note that the peak inrush value is about 35 A secondary and that the fundamental frequency component (digital filter output) magnitude is close to 15 A secondary, about 40 percent of the peak inrush value.

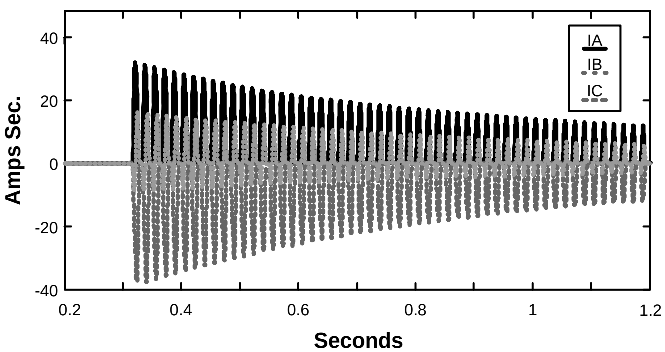

Fig. 12. Single Transformer Inrush Currents

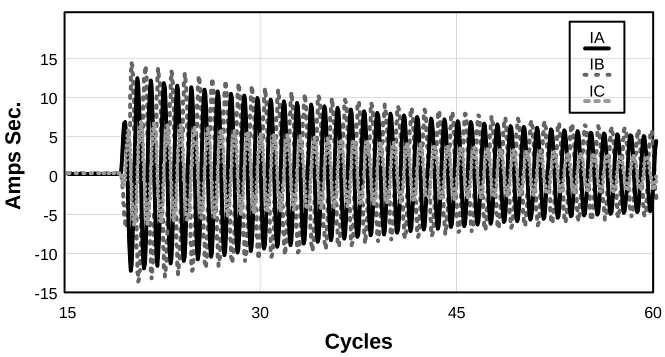

Fig. 13. Single Transformer Filtered Inrush Currents

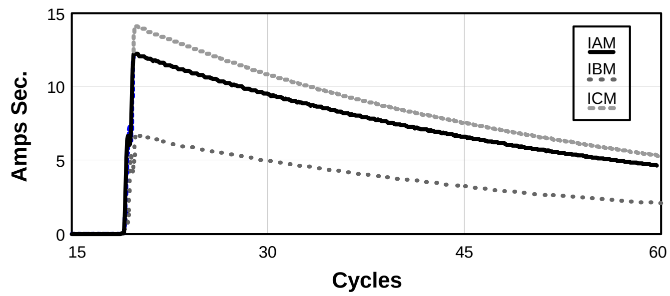

Fig. 14. Single Transformer Inrush Current Magnitudes

Fig. 15 shows the impedance plot of the distance elements. We are interested only in the phase-phase impedance plots; zero-sequence currents are insufficient to cause ground distance element operation. The plot shows two lines. The lower line (M1P) is the transformer impedance, while the other line (M2P) is an arbitrary selection showing 200 percent of the transformer impedance. Setting philosophies vary in these applications, so the figure shows these thresholds for illustrative purposes. One can see that the distance element measures a transient impedance value that is close to the transformer impedance. Overreaching Zone 2 elements can pick up on the inrush currents and trip on time delay or switch-onto-fault.

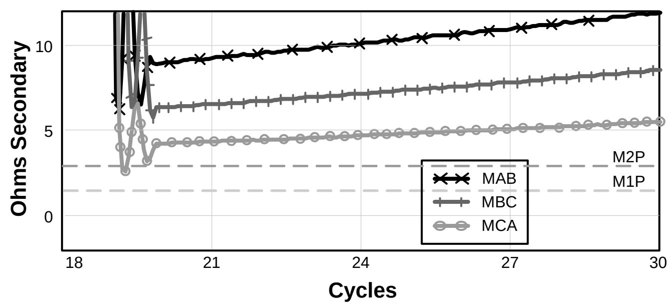

Fig. 15. Impedance Plot for Single Transformer Inrush

B. *Multiple Tapped Transformers*

The following example illustrates the distance element response to energizing a line with multiple tapped transformers. This example is similar to the previous example except that load is connected to the transformers and the impedance elements typically need to have a greater reach setting to accommodate the effects of infeed (Zone 2 elements are set typically to "see" through the transformer).

As in the previous example, the system is modeled through use of a real time digital simulator. The line is a 60-mile, 115 kV transmission line. A total of four 30 MVA, 115 kV/12.47 kV delta-wye grounded transformers are connected to the line in two locations (two transformers at each location). Each transformer feeds 10 MW of load at a 0.9 power factor; the load is connected during the line energization.

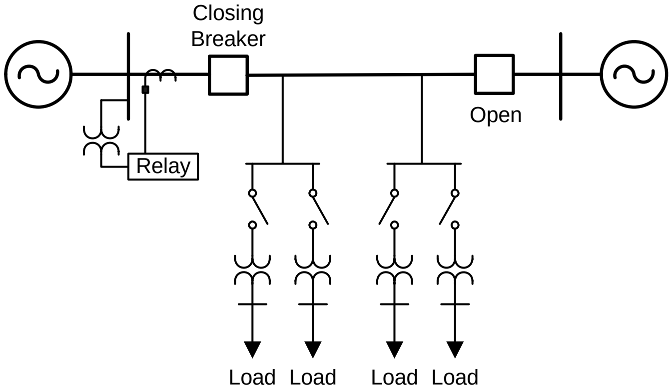

Fig. 16. Tapped Transformer System Diagram

Fig. 17 shows the inrush currents the simulator captured. Fig. 18 shows the output of the digital filter at 16 samples/cycle. Fig. 19 shows the phase current magnitudes from the digital filter output. Note that the peak inrush value is close to 12.5 A secondary and that the magnitude of the fundamental frequency component (digital filter output) is close to 4.2 A secondary, about 34 percent of the peak inrush value.

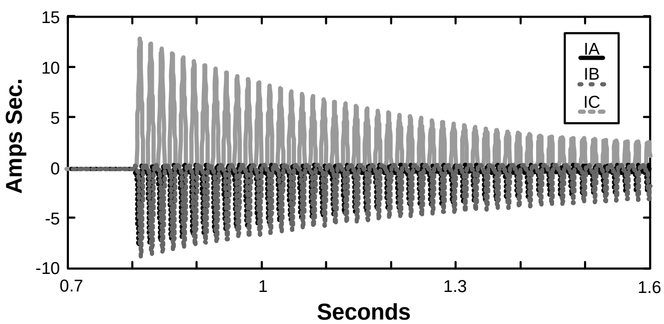

Fig. 17. Tapped Transformer Inrush Currents

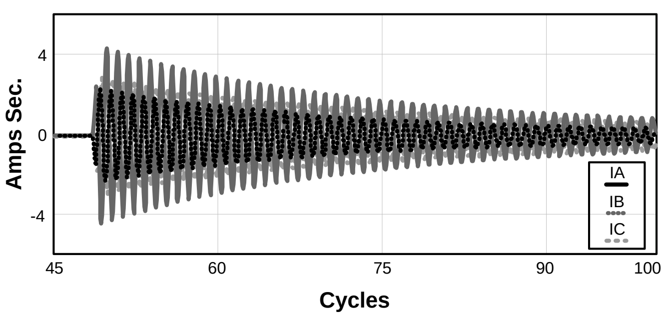

Fig. 18. Tapped Transformer Filtered Inrush Currents

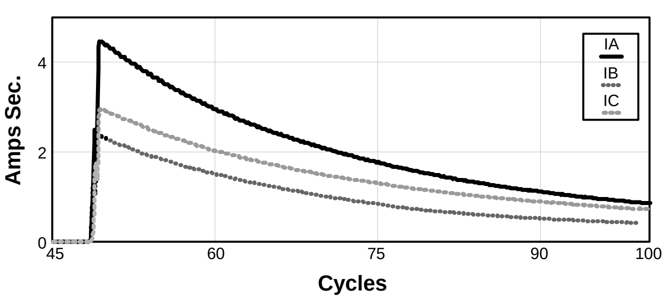

Fig. 19. Tapped Transformer Inrush Current Magnitudes

Fig. 20 shows the impedance plot of the distance elements. As with the previous example, we are interested only in the phase-phase impedance plots; zero-sequence currents are insufficient to cause ground distance element operation. The plot shows two lines. One line (M1P) shows the sum of the line impedance to the farthest connected transformer and the transformer impedance at that location. The upper line (M2P) is a typical Zone 2 distance element reach setting. The Zone 2 distance element is set to reach through the farthest transformer and include the effect of infeed from the remote terminal. The overreaching Zone 2 element is picked up for a relatively long period of time; the CA phase pair picks up for almost 20 cycles. A time delay backup element could operate for this inrush condition.

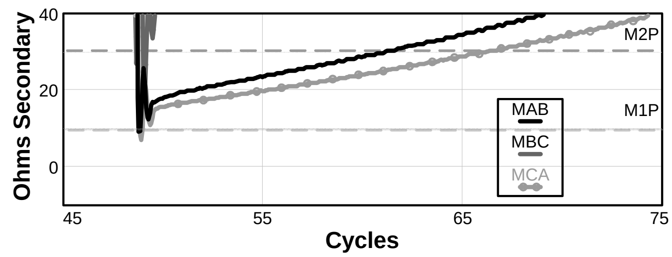

Fig. 20. Impedance Plot for Tapped Transformer Inrush

1) *Field Data*

This example shows operation of a distance element in an actual field application. The relay is connected to a 32-mile, 138 kV transmission line. The line feeds five 55 MVA transformers. The line failed to energize for three attempts (one automatic reclose and two manual closes). Line energization and load restoration occurred on the fourth attempt.

Investigation showed that the Zone 2 distance elements operated in the transformer inrush and load pickup. The following figures show the inrush currents (Fig. 21), the filtered currents (Fig. 22), and the impedance plot (Fig. 23) of one of the manual close attempts.

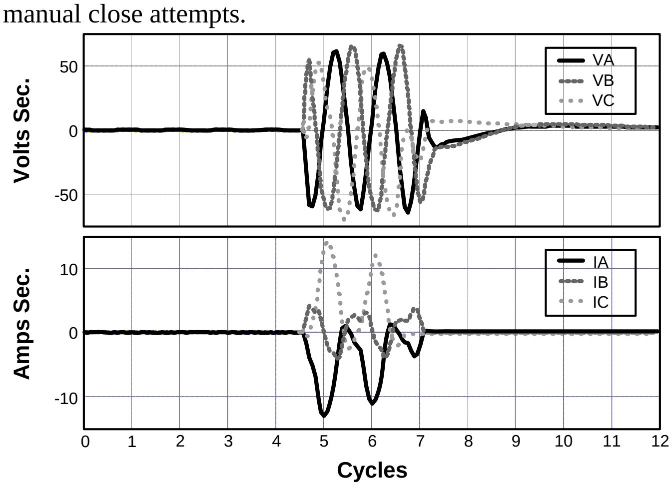

Fig. 21. Transformer Inrush Currents — Field Data

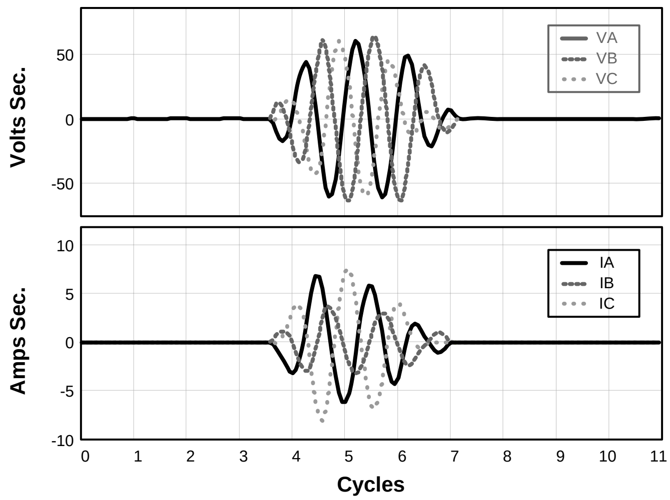

Fig. 22. Transformer Filtered Inrush Currents — Field Data

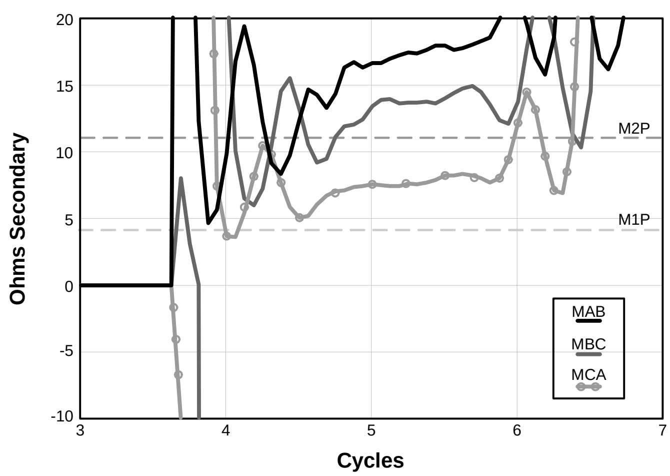

Fig. 23. Impedance Plot for Transformer Inrush — Field Data

From the impedance plot, one can see clearly that the CA phase pair impedance is well below the Zone 2 threshold. The switch-onto-fault logic is set to trip instantly on Zone 2 operation, so it is clear why the line tripped out. Although not a true representation of distance element response, an apparent impedance plot can sometimes provide useful information. Plots in Fig. 24 show the apparent phase-phase impedance and the Zone 2 steady-state mho characteristic. One can see again that the CA phase pair is well within the characteristic.

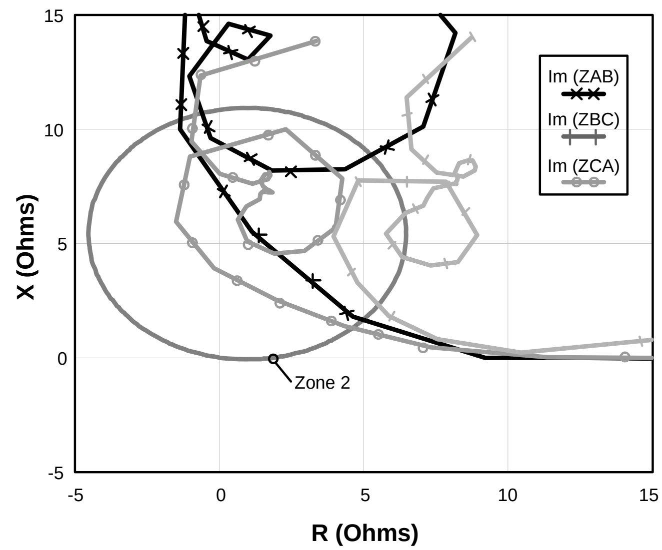

Fig. 24. Apparent Impedance Plot — Field Data

V. Recommendations

Many differing methods and guidelines exist for setting distance elements in applications involving transformers. While not exhaustive, the following recommendations serve as general guidelines and cautions for most distance element applications with transformers.

Take extra caution in setting and applying Zone 1 distance elements. There are two approaches to making a Zone 1 distance element secure in transformer applications: reduce the Zone 1 reach or apply overcurrent fault detectors. Reducing Zone 1 reach may be prohibitive in some cases, such as those applications with tapped transformers. However, in dedicated transformer applications, such reduction does not significantly impact the speed or dependability of the scheme. In other applications, set an overcurrent fault detector higher than the maximum inrush current. The simulations in this paper show that the fundamental frequency component magnitude can be easily as high as 40 percent of the maximum peak inrush current. Ensure secure Zone 1 operation by setting the overcurrent fault detector greater than this value.

It is more likely that the Zone 2 distance element can operate on inrush as a result of the increased reach setting on these overreaching elements. The Zone 2 element can cause two types of unwanted operations: switch-onto-fault or time delayed backup. For switch onto fault, supervise the Zone 2 distance element (and possibly all distance elements) with an undervoltage element. Typically, setting the undervoltage element to 75–80% of the nominal system voltage covers the majority of cases. In some applications, however, different thresholds may be necessary as a result of system conditions. For time-delayed backup applications, longer time delays may be necessary. Predicting the necessary delay can be difficult, but 0.5–0.75 seconds should be adequate in most cases.

VI. Conclusions

1. Digital filters reject harmonics and extract the fundamental frequency component of the waveform.

2. An inrush current consists of many harmonics. Monitoring these harmonics can help indicate inrush conditions versus fault conditions. The inrush current also contains a significant fundamental frequency component that a distance element will see as an operating current.
3. Distance relays applied on transformers or lines with tapped transformers can operate on inrush currents.
4. One must take precautions to ensure secure distance element operation when a relay is subjected to inrush current. Properly set fault detectors, distance element reach settings, and time delays can ensure secure operation.

VII. References

[1] E. O. Schweitzer III, D. Hou, "Filtering for Protective Relays," *Proceedings of the 19th Annual Western Protective Relay Conference*, Spokane, WA, October 20–22, 1992.

[2] E. O. Schweitzer III, J. Roberts, "Distance Relay Element Design," *Proceedings of the 19th Annual Western Protective Relay Conference*, Spokane, WA, October 20–22, 1992.

VIII. Biographies

Joe Mooney, P.E. received his B.S. in Electrical Engineering from Washington State University in 1985. He joined Pacific Gas and Electric Company upon graduation as a System Protection Engineer. In 1989, he left Pacific Gas and Electric and was employed by Bonneville Power Administration as a System Protection Maintenance District Supervisor. In 1991, he left Bonneville Power Administration and joined Schweitzer Engineering Laboratories as an Application Engineer. Shortly after starting with SEL, he was promoted to Application Engineering Manager where he remained for nearly three years. He is currently the manager of the Transmission Engineering Group of the Research and Development department at Schweitzer Engineering Laboratories. He is a registered Professional Engineer in the State of California and Washington.

Satish Samineni received his B.E degree in electrical and electronics engineering from Andhra University College of Engineering, Visakhapatnam, India. He received his Master's degree in Electrical Engineering from University of Idaho, USA, in 2003. Since 2003 he has been with Schweitzer Engineering Laboratories, Inc. in Pullman, USA, where he presently holds the position of Power Engineer. His research interests include power electronics and drives, power system protection, synchrophasor-based control applications, and power system stability.

20070131
TP6268-01